

Investigation of terminal olefine in the isothiocyanatotolane liquid crystals with alkoxy end group

Juanli Li, Zenghui Peng, Ran Chen, Jian Li, Minggang Hu, Lu Zhang & Zhongwei An


To cite this article: Juanli Li, Zenghui Peng, Ran Chen, Jian Li, Minggang Hu, Lu Zhang & Zhongwei An (2018): Investigation of terminal olefine in the isothiocyanatotolane liquid crystals with alkoxy end group, Liquid Crystals, DOI: [10.1080/02678292.2018.1449026](https://doi.org/10.1080/02678292.2018.1449026)

To link to this article: <https://doi.org/10.1080/02678292.2018.1449026>




Published online: 07 Mar 2018.



Submit your article to this journal 



View related articles 



View Crossmark data 



Investigation of terminal olefine in the isothiocyanatotolane liquid crystals with alkoxy end group

Juanli Li^{a,b}, Zenghui Peng^c, Ran Chen^d, Jian Li^{a,b}, Minggang Hu^{a,b}, Lu Zhang^{a,b} and Zhongwei An^{a,b,d}

^aState Key Laboratory of Fluorine & Nitrogen Chemicals, Xi'an, P. R. China; ^bOptical and Electrical Material Center, Xi'an Modern Chemistry Research Institute, Xi'an, P. R. China; ^cState Key Laboratory of Applied Optics, Changchun Institute of Optics, Fine Mechanics and Physics, Chinese Academy of Sciences, Changchun, P. R. China; ^dSchool of Materials Science and Engineering, Shaanxi Normal University, Xi'an, P. R. China

ABSTRACT

Three series of liquid crystals based on isothiocyanatotolane core with terminal alkenoxy groups (**4A-1-4C-2**) have been synthesised via multi-step reactions. Their thermotropic mesophases and physical properties are evaluated by comparison with the alkoxy analogues (**4a-1-4c-2**). The results show that the isothiocyanatotolane LCs with alkenoxyl terminals deliver higher birefringence (0.410~0.436), lower melting points, lower melting enthalpies and viscosity. The effects of the alkenoxy terminal groups and the lateral fluoro substituents on the mesomorphic behaviour and physical properties are discussed. The formulation of the mixture containing isothiocyanatotolane liquid crystals with alkenoxyl terminals provides evidence of an useful candidate for liquid crystal photonics.

ARTICLE HISTORY

Received 2 February 2018
Accepted 3 March 2018

KEYWORDS

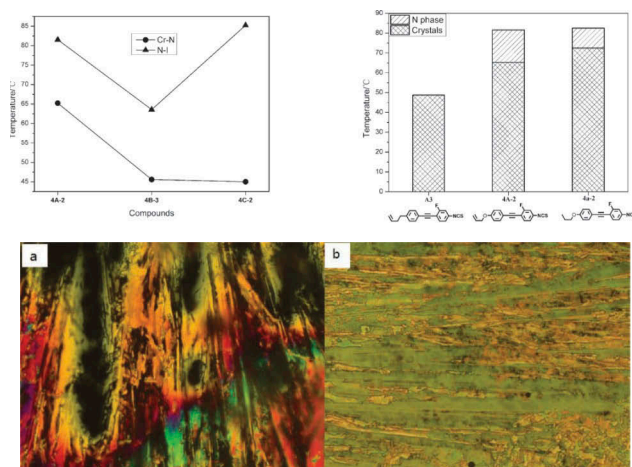
Isothiocyanatotolanes;
alkenoxy group;
birefringence; melting point;
rotational viscosity



4A-1: R=allyl, X=F, Y=H, Z=H
4A-2: R=allyl, X=H, Y=F, Z=H
4B-1: R=but-1-enyl, X=H, Y=H, Z=H
4B-2: R=but-1-enyl, X=F, Y=H, Z=H
4B-3: R=but-1-enyl, X=H, Y=F, Z=H
4B-4: R=but-1-enyl, X=F, Y=H, Z=F
4C-1: R=pent-1-enyl, X=F, Y=H, Z=H
4C-2: R=pent-1-enyl, X=H, Y=F, Z=H

4a-1: R'=n-propyl, X=F, Y=H, Z=H
4a-2: R'=n-propyl, X=H, Y=F, Z=H
4b-1: R'=n-butyl, X=H, Y=H, Z=H
4b-2: R'=n-butyl, X=F, Y=H, Z=H
4b-3: R'=n-butyl, X=H, Y=F, Z=H
4b-4: R'=n-butyl, X=F, Y=H, Z=F
4c-1: R'=n-pentyl, X=F, Y=H, Z=H
4c-2: R'=n-pentyl, X=H, Y=F, Z=H

1. Target compounds and the comparison structures.



2. By introduction of alkenoxy terminal chain and suitable lateral fluorine substitute, the properties of the target compounds **4A-1-4C-2** could be improved.

1. Introduction

Liquid crystal (LC) photonics such as spatial light modulators [1,2], laser beam steering [3], directional reflectors [4], tunable focus lenses [5], radio frequency applications in the GHz and THz spectrum [6–9], request much higher birefringence (Δn) LCs than that of common LCs in LC displays. One key concern for high Δn LCs is that the multi-unsaturated rings in the molecular skeleton can obtain LCs with large Δn (0.4–0.8), however, the undesirable functions arise out of the poor solubility, high melting point and large viscosity.

Previously, various structures including isothiocyanato derivatives of phenyl tolane [10,11], tolanyl benzene [12], bistolane [13–18] and biphenyl-bistolane [19] were developed. Molecular structure–property relationship of these LCs showed that combination of the tolane with NCS group is favourable for high Δn (>0.3) and low viscosity [20–22]. In our previous work, new but-3-enyl-based isothiocyanate LCs with a tolane core possessed high Δn (~ 0.4), low melting point, low rotational viscosity and good solubility, except for their narrow nematic phase interval [23]. Recently, it has been reported that the intermolecular actions, such as π – π stacking, dipole–dipole or hydrogen bond interactions, are the main driving forces to form the LC phase [24]. The allyloxy moieties improved the π – π stacking and dipole–dipole interactions of LCs to obtain a low melting point and broad nematic phase interval [25,26].

Against such a background, the novel alkenoxy-based tolane-LCs with NCS group may be an attractive subject for LCs with a large Δn , good solubility, low rotational viscosity and broad nematic phase interval. Meanwhile, we expect to introduce lateral fluoro-substituent into the molecular structure for further understanding molecular structure–property relationship.

Herein, eight alkenoxy-terminated isothiocyanatotolanes **4A-1–4C-2** (see Figure 1) were prepared. The reference compounds **4a-1–4c-2** were synthesised by using the reported method [27]. The effects of terminal group, lateral fluorine on the mesomorphism and physical properties of these compounds were discussed. Meanwhile, DFT calculations of molecular conformation and polarisability were also used to correlate the experimental findings.

2. Experiment

2.1. Materials

Allyl bromide, 4-bromo-1-butene and 5-bromo-1-pentene were purchased from J&K Scientific Ltd. Ethynyltrimethylsilane and 4-iodophenol was purchased from Shanghai Bangcheng Chemical Co. Ltd. 4-Iodoaniline, 2-fluoro-4-iodoaniline, 3-fluoro-4-iodoaniline were purchased from Shanghai Zhuorui Chemical Co. Ltd. 2,6-Difluoro-4-iodoaniline was purchased from Shanghai Synasst Chemical Co. Ltd. Triethylamine, copper(I)iodide, bis(triphenylphosphine)palladium(II) chloride, triphenylphosphine, and thiophosgene were purchased from TCI Chemical Reagent Co.

2.2. Characterisation

The ^1H -nuclear magnetic resonance (^1H NMR) spectra were recorded on a Bruker AV500 (500 MHz) instrument using tetramethylsilane (TMS) as internal standard. IR spectra were recorded using a Nicolet Avatar360E spectrometer. The mass spectra (MS) were obtained by GC/MS Thermo DSQ with m/z 50–650. Polarising optical micrographs (POM) were recorded on an Olympus BX51 equipped with a Mettler HS82 heating stage and HS1 temperature con-

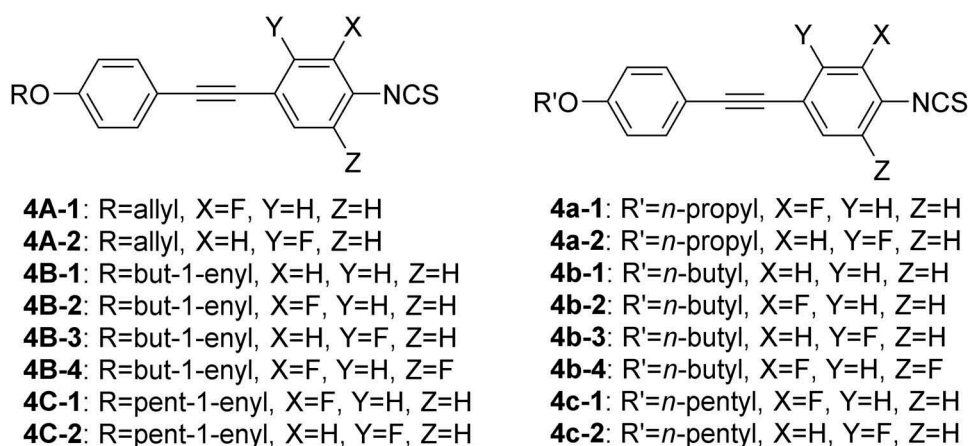
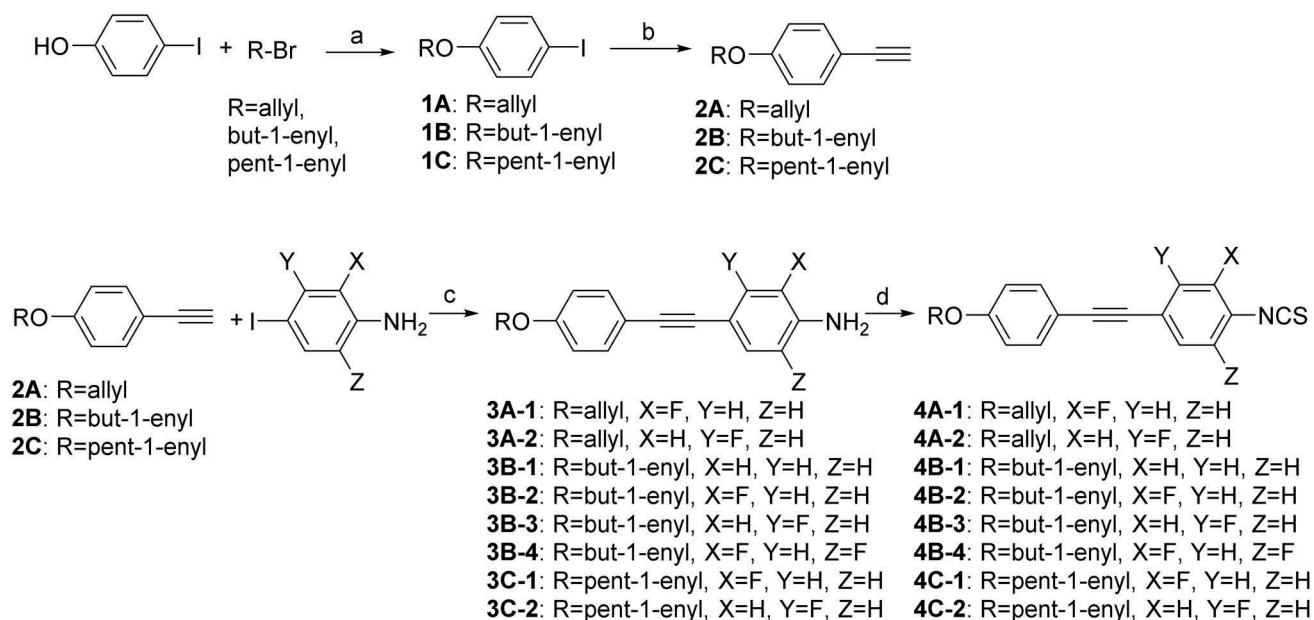


Figure 1. Target compounds and the comparison structures.



Scheme 1. Synthetic route of compounds **4A-1-4C-2**. (a) K_2CO_3 , EtOH, reflux, 2 h, (80–82%). (b) 1. $Pd(PPh_3)_2Cl_2$, CuI, PPh_3 , Et_3N , TMSA, $40^\circ C$, 3 h; 2. KOH, EtOH, $25^\circ C$, 1 h, (81–85%). (c) $Pd(PPh_3)_2Cl_2$, CuI, PPh_3 , Et_3N , $70^\circ C$, 4 h, (69–75%). (d) $CSeCl_2$, acetone, H_2O , $25^\circ C$, 1 h, (68–82%).

trol unit. The transition temperatures were confirmed by DSC analysis (DSC1) in nitrogen at heating and cooling rate of $5^\circ C/min$.

The dielectric anisotropies ($\Delta\epsilon$) were measured by an electrical constants instrument (EC-1, TOYO Corporation, Japan). The viscosity (γ_1) was measured by a Model 6254 (multi-channel liquid crystal evaluation system, TOYO Corporation, Japan). The birefringence (Δn) values were measured by an Abbe refractometer using a 589 nm wavelength light source. All of the measurements were carried out at $25^\circ C$. The physical properties of the single compound were obtained from 5 wt% solutions in the host mixture P0 (with melting point of $6^\circ C$, clearing point of $112.7^\circ C$, dielectric anisotropy of 5.63, birefringence value of 0.08) [28] by extrapolation. DFT computational studies based on quantum mechanical calculations were performed without imposing any constraints using the Gaussian 09 programme package. Spin-restricted DFT calculations were carried out in the framework of the generalised gradient approximation (GGA) using B3LYP exchange-correlation functional and the 6-311G (d, p) basis set [29].

2.3. Synthesis

The new alkenoxy-based isothiocyanatotolane compounds **4A-1-4C-2** were prepared using the route shown in Scheme 1.

2.3.1. Synthesis of 1-(but-3-en-1-yloxy)-4-iodobenzene (1B)

A mixture of 4-iodophenol (39.6 g, 0.18 mol), 4-bromobut-1-ene (36.5 g, 0.27 mol), potassium carbonate (49.7 g, 0.36 mol) and 200 mL of ethanol was heated at reflux for 2 h. After cooling the mixture to room temperature, the ethanol was separated and then 300 mL of *n*-heptane was added. Then the organic layer was washed with water and dried over anhydrous $MgSO_4$. The crude product was isolated by evaporating the solvent, and purified by column chromatography using *n*-heptane as eluent to give a light yellow liquid with a yield of 82% and purity of 98.53%. 1H NMR ($CDCl_3$, 500 MHz) δ (ppm): 2.509–2.549 (q, 2H), 3.958–3.984 (t, 2H), 5.099–5.183 (m, 2H), 5.843–5.925 (m, 1H), 6.660–6.690 (m, 2H), 7.526–7.556 (m, 2H); IR (KBr, cm^{-1}): 3077, 2978, 2924, 2874, 2524, 1872, 1572, 1486, 1430, 1282, 1113, 1032, 918, 819; MS m/z (RI, %): 274.0 (M^+ , 74), 246.0 (34), 220.0 (100), 203.0 (13), 191.0 (5), 93.0 (8), 55.1 (9).

2.3.2. Synthesis of 1-(but-3-en-1-yloxy)-4-ethynylbenzene (2B)

Ethynyltrimethylsilane (35 g, 0.36 mol) in triethylamine was added dropwise to a suspension of **1B** (49 g, 0.18 mol), $Pd(PPh_3)_2Cl_2$ (0.63 g, 0.9 mmol), copper(I)iodide (0.52 g, 2.7 mmol) and triphenylphosphine (0.73 g, 2.7 mmol) in 250 mL of triethylamine at $40^\circ C$ under nitrogen. The solution was stirred for 3 h.

The mixture was filtered and the filtrate was concentrated to remove triethylamine. The crude product was dissolved in *n*-heptane and purified by column chromatography using *n*-heptane as eluent to give a yellow liquid (40 g).

A mixture of the yellow liquid and potassium hydroxide (5.2 g, 0.09 mol) in ethanol (250 mL) was stirred at room temperature for 1 h. Then *n*-heptane was added and the organic layer was washed with water, dried over anhydrous MgSO_4 . After evaporating the solvents, a red liquid was given, yield 84% with purity of 98.7%. ^1H NMR (CDCl_3 , 500 MHz) δ (ppm): 2.518–2.564 (m, 2H), 2.988 (s, 1H), 4.000–4.027 (t, 2H), 5.098–5.190 (m, 2H), 5.851–5.933 (m, 1H), 6.819–6.848 (m, 2H), 7.401–7.429 (m, 2H); IR (KBr, cm^{-1}): 3078, 3043, 2980, 2873, 2314, 2107, 1892, 1642, 1606, 1506, 1289, 1171, 1032, 920, 833, 810; MS m/z (RI, %): 172.0 (M^+ , 55), 118.0 (100), 144.0 (18), 89.0 (13), 75.0 (5), 55.1 (12).

2.3.3. Synthesis of 4-((4-(but-3-en-1-yloxy)phenyl)ethynyl)-2-fluoroaniline (3B-2)

2-Fluoro-4-iodoaniline (25.36 g, 0.107 mol), $\text{Pd}(\text{PPh}_3)_2\text{Cl}_2$ (0.75 g, 1.07 mmol), triphenylphosphine (0.84 g, 3.21 mmol), copper(I)iodide (0.61 g, 3.21 mmol) and triethylamine (200 mL) were mixed under nitrogen. A solution of compound **2B** (20.32 g, 0.118 mol) dissolved in 30 mL of triethylamine was added dropwise and the mixture stirred at 70°C for 4 h. The mixture was filtered and the filtrate was concentrated to remove triethylamine. The crude product was dissolved in toluene and washed with water and dried over anhydrous MgSO_4 . After removal of the solvent in vacuum, the residue was recrystallised two times from the mixing solution of *n*-heptane (20 mL) and toluene (20 mL) at -20°C to obtain **3B-2** as light yellow crystals, yield 71% with purity of 99.28%. M.p.: 83.03–84.33°C; ^1H NMR (CDCl_3 , 500 MHz) δ (ppm): 2.529–2.570 (m, 2H), 3.855 (s, 2H), 4.012–4.039 (t, 2H), 5.104–5.197 (m, 2H), 5.862–5.943 (m, 1H), 6.689–6.724 (q, 1H), 6.841–6.869 (m, 2H), 7.095–7.154 (m, 2H), 7.400–7.428 (m, 2H); IR (KBr, cm^{-1}): 3480, 3391, 3068, 2978, 2863, 2207, 1632, 15188, 1427, 1193, 1105, 984, 859; MS m/z (RI, %): 281.0 (M^+ , 98), 227.0 (100), 198.0 (17), 170.0 (6), 151.0 (4), 55.1 (2).

2.3.4. Synthesis of 4-((4-(but-3-en-1-yloxy)phenyl)ethynyl)-2-fluoro-1-isothiocyanatobenzene (4B-2)

A solution of the prepared **3B-2** (11.53 g, 0.041 mol), thiophosgene (5.75 g, 0.05 mol), acetone (50 mL) and 5 mL of water was stirred for 1 h at room temperature. The mixture was concentrated in vacuum to remove acetone, and *n*-heptane (50 mL) was added. The mixture was washed with water and dried over anhydrous MgSO_4 . After removal of the solvent, the crude product

was purified on a chromatographic column filled with silica gel by using *n*-heptane as eluent. The eluent was concentrated to dryness and the solid was crystallised at -20°C from *n*-heptane (100 mL); final yield 10.6 g (80%) with purity of 99.78%. ^1H NMR (CDCl_3 , 500 MHz) δ (ppm): 2.537–2.577 (m, 2H), 4.025–4.052 (t, 2H), 5.111–5.201 (m, 2H), 5.861–5.943 (m, 1H), 6.866–6.895 (m, 2H), 7.117–7.148 (t, 1H), 7.221–7.298 (m, 2H), 7.428–7.456 (m, 2H); IR (KBr, cm^{-1}): 3083, 3052, 2997, 2929, 2876, 2209, 2016, 1558, 1516, 1464, 1204, 1105, 1029, 926, 831, 764; MS m/z (RI, %): 323.0 (M^+ , 72), 269.0 (100), 239.9 (7), 208.0 (7), 181.0 (8), 55.1 (5).

4A-1: The same procedure as **4B-2**, an amount of 9.8 g compound **4A-1** was obtained with yield of 82% and purity of 99.60% (GC). ^1H NMR (CDCl_3 , 500 MHz) δ (ppm): 4.557–4.573 (m, 2H), 5.302–5.325 (m, 1H), 5.405–5.443 (m, 1H), 6.025–6.081 (m, 1H), 6.891–6.909 (m, 2H), 7.119–7.151 (t, 2H), 7.224–7.285 (m, 1H), 7.437–7.455 (m, 2H); IR (KBr, cm^{-1}): 3081, 3018, 2916, 2856, 2201, 2061, 1567, 1516, 1450, 1247, 1104, 1021, 958, 927, 829; MS m/z (RI, %): 309.0 (M^+ , 66), 267.9 (100), 239.9 (23), 208 (10), 182 (17).

4A-2: The same procedure as **4B-2**, an amount of 4.5 g compound **4A-2** was obtained with yield of 69% and purity of 99.66% (GC). ^1H NMR (CDCl_3 , 500 MHz) δ (ppm): 4.555–4.571 (m, 2H), 5.297–5.321 (q, 1H), 5.403–5.440 (q, 1H), 6.012–6.089 (m, 1H), 6.884–6.912 (m, 2H), 6.953–7.007 (m, 2H), 7.437–7.487 (m, 3H); IR (KBr, cm^{-1}): 3088, 2919, 2863, 2218, 2118, 1612, 1555, 1515, 1422, 1248, 1168, 1012, 936, 834, 794; MS m/z (RI, %): 308.9 (M^+ , 66), 267.9 (100), 239.9 (22), 207.9 (8), 182 (16), 156 (2).

4B-1: The same procedure as **4B-2**, an amount of 5.3 g compound **4B-1** was obtained with yield of 68% and purity of 99.43% (GC). ^1H NMR (CDCl_3 , 500 MHz) δ (ppm): 2.534–2.579 (m, 2H), 4.021–4.028 (t, 2H), 4.974–5.269 (m, 2H), 5.862–5.944 (m, 1H), 6.862–6.891 (m, 2H), 7.172–7.198 (m, 2H), 7.432–7.479 (m, 4H); IR (KBr, cm^{-1}): 3081, 2979, 2939, 2874, 2214, 2091, 1604, 1514, 1465, 1249, 1173, 1033, 928, 835, 702; MS m/z (RI, %): 305.0 (M^+ , 77), 251.0 (100), 222.0 (7), 190.0 (6), 163.0 (9), 55.1 (3).

4B-3: The same procedure as **4B-2**, an amount of 6.1 g compound **4B-3** was obtained with yield of 71% and purity of 99.06% (GC). ^1H NMR (CDCl_3 , 500 MHz) δ (ppm): 2.536–2.576 (m, 2H), 4.024–4.051 (t, 2H), 5.110–5.200 (m, 2H), 5.861–5.942 (m, 1H), 6.865–6.894 (m, 2H), 6.952–7.007 (m, 2H), 7.436–7.484 (m, 3H); IR (KBr, cm^{-1}): 3063, 2980, 2940, 2882, 2217, 2086, 1551, 1515, 1465, 1245, 1101, 1059, 989, 819, 776; MS m/z (RI, %): 323.0 (M^+ , 74), 262.0 (100), 240.0 (7), 208.0 (7), 182.0 (8), 55.1 (3).

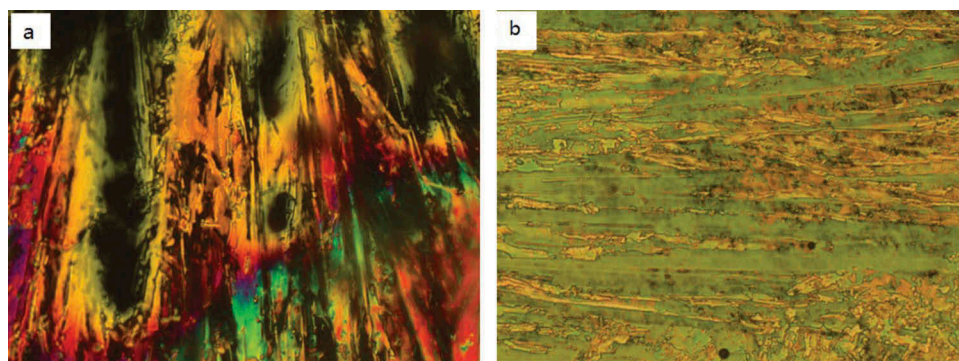


Figure 2. (Colour online) Photo micrographs ($\times 200$): (a) Nematic schlieren texture at 49.2°C in heating process. (b) Thread-like texture of the nematic mesophase at 34.5°C in heating process.

4B-4: The same procedure as **4B-2**, an amount of 8.8 g compound **4B-4** was obtained with yield of 82% and purity of 99.39% (GC). ^1H NMR (CDCl_3 , 500 MHz) δ (ppm): 2.534–2.580 (m, 2H), 4.026–4.053 (t, 2H), 5.109–5.201 (m, 2H), 5.859–5.940 (m, 1H), 6.868–6.897 (m, 2H), 7.057–7.095 (t, 2H), 7.423–7.451 (m, 2H); IR (KBr, cm^{-1}): 3087, 3065, 2982, 2941, 2871, 2197, 2015, 1564, 1512, 1429, 1244, 1115, 1042, 921, 854, 707; MS m/z (RI, %): 340.9 (M^+ , 73), 286.9 (100), 254.9 (6), 225.9 (6), 199.9 (7), 55.1 (7).

4C-1: The same procedure as **4B-2**, an amount of 10.7 g compound **4C-1** was obtained with yield of 79% and purity of 99.26% (GC). ^1H NMR (CDCl_3 , 500 MHz) δ (ppm): 1.868–1.923 (m, 2H), 2.219–2.267 (m, 2H), 3.974–4.000 (t, 2H), 4.997–5.089 (m, 2H), 5.810–5.891 (m, 1H), 6.856–6.885 (m, 2H), 7.109–7.141 (t, 1H), 7.215–7.277 (m, 2H), 7.422–7.451 (m, 2H); IR (KBr, cm^{-1}): 3076, 2922, 2866, 2202, 2075, 1598, 1513, 1419, 1247, 1104, 1023, 957, 916, 828; MS m/z (RI, %): 337.0 (M^+ , 60), 268.9 (100), 236.9 (6), 182.0 (6).

4C-2: The same procedure as **4B-2**, an amount of 5.3 g compound **4C-2** was obtained with yield of 70% and purity of 99.30% (GC). ^1H NMR (CDCl_3 , 500 MHz) δ (ppm): 1.867–1.923 (m, 2H), 2.221–2.264 (m, 2H), 3.975–4.001 (t, 2H), 4.996–5.089 (m, 2H), 5.810–5.892 (m, 1H), 6.857–6.880 (m, 2H), 6.949–7.003 (m, 2H), 7.433–7.480 (m, 3H); IR (KBr, cm^{-1}): 3075, 2948, 2870, 2217, 2116, 1565, 1552, 1456, 1252, 1106, 1029, 956, 924, 834; MS m/z (RI, %): 337.0 (M^+ , 58), 268.9 (100), 236.9 (20), 182.0 (7), 41.1 (3).

3. Results and discussion

3.1. Synthesis

In step d of NCS compounds, a different method was used. In our previous work [12,23], chloroform, calcium carbonate and water were used. Here, acetone and water were used as solvent to increase the solubility of the reactant without addition of calcium carbonate. The solvent can be removed directly without filtration.

Table 1. Types of phase transition, temperatures and associated enthalpies obtained by POM and DSC for the new compounds and the reference compounds.

Compound	Transition temperature, °C (enthalpy change, kJ/mol)		Nematic range, °C	
	Heating process	Cooling process	Heating process	Cooling process
4A-1	Cr 87.55 (28.92) I	I 75.98 (0.40) N 53.04(18.44) Cr	—	22.94
4A-2	Cr 65.23 (19.25) N 81.54 (0.49) I	I 82.04 (0.51) N 41.45 (17.28) Cr	16.31	40.59
4B-1	Cr 104.13 (21.78) I	I 97.65 (20.38) Cr	—	—
4B-2	Cr 88.39 (33.42) I	I 79.38 (36.92) Cr	—	—
4B-3	Cr 45.60 (18.89) N 63.57 (0.30) I	I 64.11 (0.28) N 22.55 (16.75) Cr	17.97	41.56
4B-4	Cr 72.53 (29.21) I	I 43.58 (26.65) Cr	—	—
4C-1	Cr 50.11 (22.82) N 78.69 (0.42) I	I 79.25 (0.43) N 35.83 (22.08) Cr	28.58	43.42
4C-2	Cr 45.02 (21.36) N 85.24 (0.5) I	I 85.73 (0.51) N 25.34 (16.68) Cr	40.22	60.39
4a-1	Cr 88.75 (31.13) I	I 79.39 (31.73) Cr	—	—
4a-2	Cr 72.51 (22.56) N 82.55 (0.401) I	I 82.93 (0.43) N 52.35 (23.39) Cr	10.04	30.58
4b-1	Cr 112.81 (23.32) N 115.65 (0.50) I	I 115.96 (0.72) N 112.13 (13.00) SmE 96.18 (8.28) Cr	2.84	3.83
4b-2	Cr 96.52 (34.35) I	I 89.97 (0.42) N 56.43 (20.18) Cr	—	33.54
4b-3	Cr 70.53 (24.79) N 94.53 (0.59) I	I 94.88 (0.56) N 48.23 (22.64) Cr	24.00	46.65
4b-4	Cr 70.22 (31.76) I	I 62.27 (0.34) N 38.72 (29.22) Cr	—	23.55
4c-1	Cr 79.57 (41.79) I	I 82.76 (0.31) N 70.00 (40.64) Cr	—	12.76
4c-2	Cr 60.95 (23.84) N 86.28(0.45) I	I 86.75 (0.49) N 31.13 (20.88) Cr	25.33	55.62

Cr: crystal; SmE: smectic E phase; N: nematic phase; I: isotropic liquid.

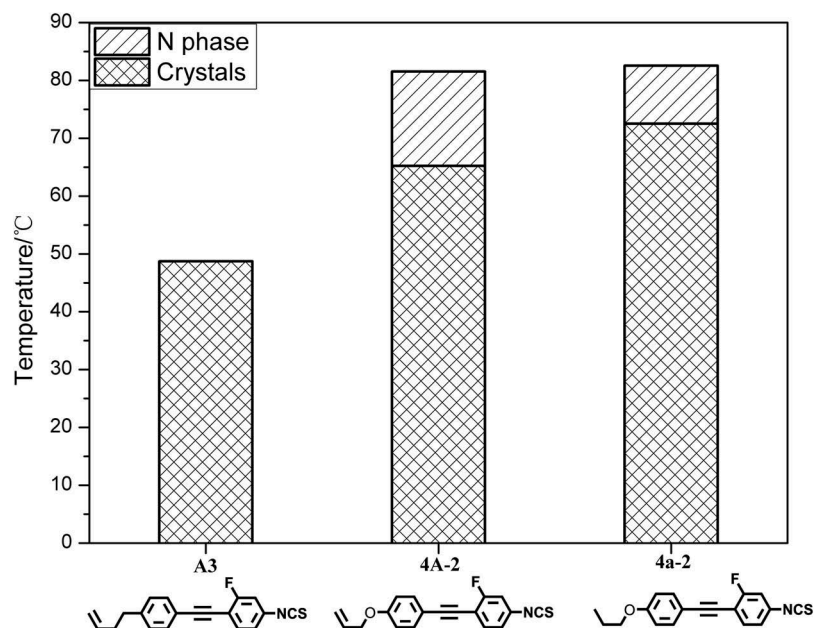


Figure 4. Transition behaviour of the compounds **A3**, **4A-2** and **4a-2**: dependence of the transition temperatures on the terminal group.

Meanwhile, the residual thiophosgene was exhausted by alkali solution while evaporating the solvent to inhibit harm of health.

3.2. Mesomorphic properties

The phase transition temperatures, the associated enthalpy changes, nematic range and mesophase textures of the investigated compounds are summarised in Table 1.

The textures of the new compounds were examined with POM. The observed phase transitions were identical with those from DSC curves. The POM micrographs of compounds **4B-3** are given in Figure 2.

3.2.1. The effect of the alkenoxy terminal chain on the mesomorphic properties

As shown in Table 1, except for **4B-4**, these new LCs exhibit lower melting point (45.02~104.14°C) than those of their analogous compounds (60.95~112.81°C). All of these LCs show lower melting enthalpies (18.89~33.42 kJ/mol) than those of the analogous compounds (22.56~41.79 kJ/mol). These results indicate that replacement of alkoxy chain by alkenoxy as terminal group brings lower melting point and melting enthalpies, owing to the weaker lattice energy of molecules **4A-1** – **4C-2**. Hence, these compounds exhibit good miscibility, which is favourable to improve the solubility in

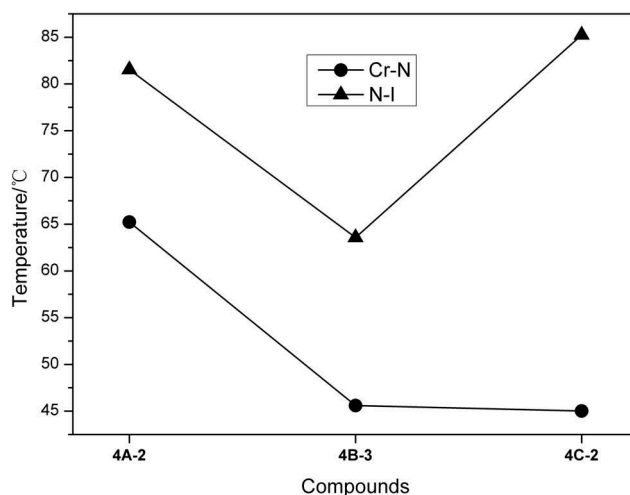


Figure 3. Transition behaviour of the compounds **4A-2**, **4B-3** and **4C-2**: dependence of the transition temperatures on the carbon number of the terminal alkenoxy chain.

LC mixtures. In addition, compared the new compounds with their corresponding analogous structures, there is evidence that the replacing odd alkoxy terminal chains with odd alkenoxy terminal chains can enhance the stability of the nematic phase. As for compounds **4A-1** and **4B-2** with shorter terminal chain, show no LC phase, while the analogues **4C-1** and **4C-2** with longer terminal chain exhibit a nematic phase, which is also observed in our previous paper [12].

Figure 3 presents the transition temperatures of compounds **4A-2**, **4B-3** and **4C-2** with fluorine substitute in site Y, in the heating process, as a function of the number of carbon atoms in the alkyl chain. The length of the alkyl chain affects not only the melting points but also clearing points. Their melting points show a downward tendency with increasing alkyl chain, while the nematic phase temperature ranges show an upward tendency, which indicates that the longer the terminal chains are, the wider the nematic phase ranges of the analogues (**4A-2**, **4B-3** and **4C-2**) are. It shows odd-even effect for the clearing points of **4A-2**, **4B-3** and **4C-2**, compounds **4A-2** and **4C-2** with odd terminal chains exhibit higher clearing points than those with even terminal chains (**4B-3**).

As shown in Figure 4, but-3-enyl-based isothiocyanatetotolane LC (**A3**) [23] shows no mesomorphous phase, and compound **4a-2** with propoxy terminal group exhibits a narrow nematic phase range of 10.04°C, while allyloxy-based compound **4A-2** show a

nematic phase interval of 16.31°C. These results indicate that the allyloxy group improves the dipole–dipole or π – π stacking interactions to enhance nematic phase interval.

3.2.2. The effect of the lateral fluorine on the mesomorphic properties

In Figure 5, among series **4B**, only **4B-3** with lateral fluorine at Y position displays a nematic phase. Compound **4B-1** without lateral fluorine exhibits the highest melting point of 104.13°C. After introduction of lateral fluorine into the X position, the melting point falls down to 88.39°C. Meanwhile, introduction of lateral fluorine into the Y position reduces melting point of 45.6°C. Introduction of lateral difluorine substitutes into the X and Z positions increases the melting point to 72.53°C. Comparing compounds **4A-1** and **4C-1** with **4A-2** and **4C-2**, we also find that the compounds with fluorine at the Y position have lower melting point and broader nematic phase temperature range than those of the compounds with fluorine at the X position, which indicates that lateral fluorine at the Y position can decrease the melting point and enhance nematic phase interval. As observed in Figure 6, the simulated molecular structures present that the dipole moment μ in **4B-2** with fluorine at the X position is 5.86, while the μ in **4B-3** with fluorine at the Y position is down to 4.63, which reveals that lateral fluorine at the Y position decreases the dipole–dipole interactions to benefit the stability of nematic phase.

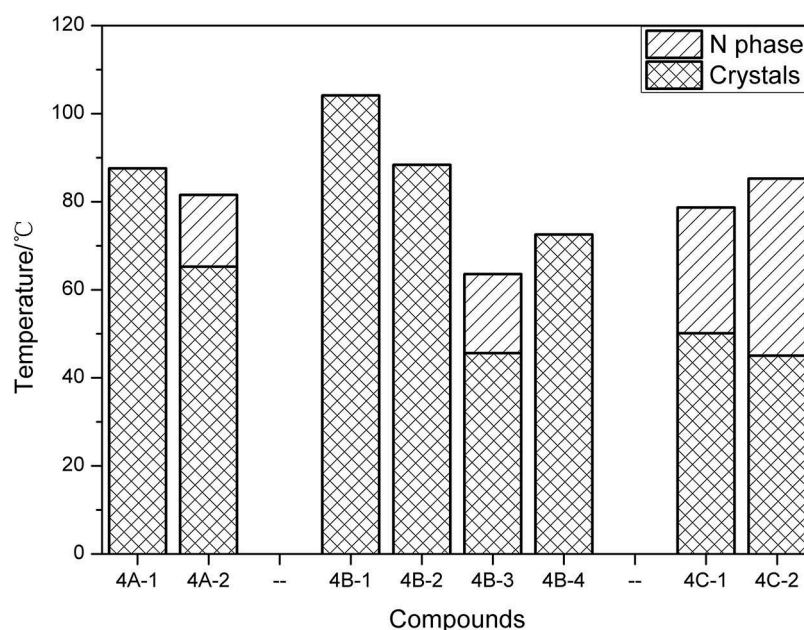


Figure 5. The effect of lateral fluorine substitute on the mesomorphism.

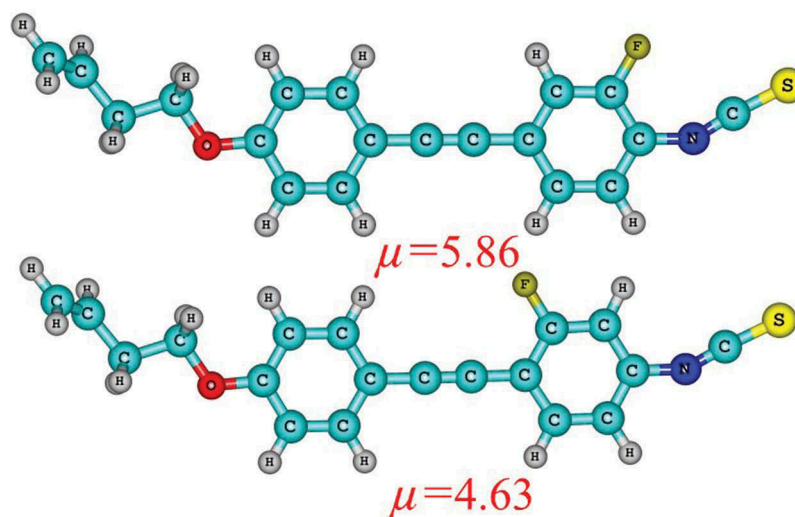


Figure 6. (Colour online) Molecular structures of compounds **4B-2** (up) and **4B-3** (bottom) optimised at the DFT/b3lyp/6-311G (d, p) level of theory.

Table 2. The electro-optical properties^b and DFT calculated principal components (α_{xx} , α_{yy} , α_{zz}), isotropic component $\alpha = (\alpha_{xx} + \alpha_{yy} + \alpha_{zz})/3$, anisotropy $\Delta\alpha = [\alpha_{xx} - (\alpha_{yy} + \alpha_{zz})/2]$, dipole moment (μ) of compounds **4B-1**, **4B-2**, **4B-3**, **4B-4**, and **4b-3**^a.

compd.	α_{xx}	α_{yy}	α_{zz}	α	$\Delta\alpha$	μ	Δn^b	$\Delta\epsilon^b$	γ_1^c (mPa s)
4B-1	648.1	201.3	113.1	320.8	490.9	5.38	0.436	16.95	143.7
4B-2	645.1	204.6	113.2	321.0	486.2	5.86	0.424	23.25	141.1
4B-3	649.9	203.5	113.2	322.2	491.6	4.63	0.420	12.11	144.7
4B-4	650.6	204.8	113.2	322.9	491.6	6.79	0.410	28.19	147.6
4b-3	653.9	205.5	112.2	323.9	495.1	5.02	0.398	14.95	151.1

^a All polarisability components and the anisotropy parameter are expressed in Bohr ³ (with 1 Bohr = 0.52917 Å); ^b Experimental measurement results; ^c 95 wt% P0 + 5 wt% single compound.

3.3. Structure–property relationship

In order to investigate the structure–property relationship of these new LCs, **4B-1**, **4B-2**, **4B-3**, **4B-4**, and **4b-3** were selected to dissolve in a host mixture P0. Then, the Δn and the $\Delta\epsilon$ of these compounds can be extrapolated according to the following equations [30,31]:

$$(\Delta n)_{gh} = x(\Delta n)_g + (1-x)(\Delta n)_h \quad (1)$$

$$(\Delta\epsilon)_{gh} = x(\Delta\epsilon)_g + (1-x)(\Delta\epsilon)_h \quad (2)$$

where gh , g , and h is the birefringence and dielectric anisotropy value of the guest–host system, guest compound, and host mixture, respectively. Their physical properties, molecular polarisabilities and dipole moments are shown in Table 2.

Table 2 presents that these new LCs possess high Δn and large $\Delta\epsilon$, while the effect of lateral fluorine substitute shows an obvious difference. The Δn values show a downward tendency with increasing lateral fluorine substitutes, meanwhile the suitable fluorine substitute would increase $\Delta\epsilon$. Compared to the butoxy-based LC **4b-3**, the but-3-enyloxy-based LC **4B-3** reveals a higher Δn and lower $\Delta\epsilon$ value. From [32], the birefringence and dielectric anisotropy of a nematic liquid crystal mostly depend on the polarisability anisotropy $\Delta\alpha$ and dipole moment μ , which can explain the numerical relationship of Δn and $\Delta\epsilon$ for these compounds with the same molecular skeleton. However, some compounds possess a high $\Delta\alpha$ value, but reveals a low Δn value. It is noted that the birefringence is analysed using the Vuks equation [33], which is related with order parameter S of molecules. For example,

Table 3. Test mixtures and their properties.

Mixture	Compositions	Δn (25°C, 589 nm)	$\Delta\epsilon$	$T_{m.p.}/^\circ\text{C}$	$T_{c.p.}/^\circ\text{C}$	γ_1 (25°C)/mPa s	Low temperature storage
Host1	61 wt% (Tolane isothiocyanates) + 18 wt% (phenyl tolane isothiocyanates) + 21 wt% (cyclohexyl tolane isothiocyanates)	0.3991	15.9	−26.3	101.9	239.9	−16°C, Smectic
Mix-1	Host1 + 10 wt% (4A-1 + 4A-2)	0.4028	16.1	−27.1	98.4	197.0	−16°C, Nematic
Mix-2	Host1 + 10 wt% (4a-1 + 4a-2)	0.4011	17.1	−24.0	101.5	221.0	−16°C, Smectic

compound **4B-1** with a higher order parameter to obtain the higher Δn , while the lateral fluorine decreases the order parameter S of compound **4B-3**, thereby resulting in its lower birefringence, which explain why **4B-1** exhibits a larger Δn value than that of **4B-3**.

In Table 2, compound **4B-3** shows lower rotational viscosity than that of the compound **4b-3**, which indicates that the terminal alkenoxy chains are effective to decrease the viscosity. Meanwhile, compound **4B-2** with fluorine at the X position shows the lowest viscosity among those of other analogous compounds **4B-1**, **4B-3** and **4B-4**, which shows that the suitable lateral fluorine substitute would obtain low-viscosity LC.

3.4. High birefringence mixtures

In order to formulate high birefringence mixtures with low melting temperatures, we chose one host mixture named Host1 as bench marks for comparisons. It was formulated by phenyl tolane series, cyclohexyl tolane series and tolane isothiocyanate LCs. The mixtures were formulated by doping different series of compounds (**4A-1**, **4A-2** and **4a-1**, **4a-2**) with the same amount. Their compositions and physical properties are presented in Table 3.

Compared with **Mix-2**, **Mix-1** exhibits slightly higher Δn values, lower melting points, lower rotational viscosity and improved low temperature stability. Therefore, we believe that new allyloxy-based compounds are effective to broaden the nematic phase range, especially to decrease the melting point and the rotational viscosity of the high birefringence mixtures.

4. Conclusions

Three new series of alkenoxy-terminated isothiocyanatotolane compounds were synthesised and their structures confirmed via spectroscopic methods. Measurements of DSC and POM show that terminal olefine not only increases Δn and broadens nematic phase temperature intervals, but also decreases the melting points, melting enthalpies and rotational viscosity compared with their saturated alkoxy compounds. In addition, the odd alkenoxy terminal groups and the lateral fluoro substituent at the Y position benefit the stability of the nematic phase. Compared with but-3-enyl or propoxy terminal group, the allyloxy group improves the dipole-dipole or π - π stacking interactions to enhance the nematic phase interval. Our preliminary results confirm that alkenoxy-terminated isothiocyanatotolane LCs improve properties of high Δn LC mixtures significantly.

Disclosure statement

No potential conflict of interest was reported by the authors.

Funding

This work was supported by the the Defence Industrial Technology Development Program of China [Grant Number JSHS2015208B005]; the State Key Laboratory of Applied Optics [Grant Number Y6133FQ112]; the National Natural Science Foundation of China [Grant Number 61378075].

References

- [1] Huang Y, He Z, Wu ST. Fast-response liquid crystal phase modulators for augmented reality displays. *Opt Express*. 2017;25:32757–32766.
- [2] Jesacher A, Maurer C, Schwaighofer A, et al. Near-perfect hologram reconstruction with a spatial light modulator. *Opt Express*. 2008;16:2597–2603.
- [3] Khan SA, Riza NA. Demonstration of 3-dimensional wide angle laser beam scanner using liquid crystals. *Opt Express*. 2004;12:868–882.
- [4] Bowley CC, Yuan H, Crawford GP. Morphology of holographically-formed polymer dispersed liquid crystals (H-PDLC). *Mol Cryst Liq Cryst*. 1999;331:209–216.
- [5] Ren HW, Fan YH, Gauza S, et al. Tunable-focus flat liquid crystal spherical lens. *Appl Phys Lett*. 2004;84:4789–4791.
- [6] Li XF, Tan N, Pivnenko M, et al. High-birefringence nematic liquid crystal for broadband THz applications. *Liq Cryst*. 2016;43:955–962.
- [7] Wegłowska D, Kula P, Herman J. High birefringence bistolane liquid crystals: synthesis and properties. *RSC Adv*. 2015;6:403–408.
- [8] Vieweg N, Jansen C, Shakfa MK, et al. Molecular properties of liquid crystals in the terahertz frequency range. *Opt Express*. 2010;18:6097–6107.
- [9] Vieweg N, Koch M. Terahertz properties of liquid crystals with negative dielectric anisotropy. *Appl Optics*. 2010;49:5764–5767.
- [10] Gauza S, Wang H, Wen CH, et al. High birefringence isothiocyanato tolane liquid crystals. *Jpn J Appl Phys*. 2003;42:3463–3466.
- [11] Peng ZH, Wang QD, Liu YG, et al. Electrooptical properties of new type fluorinated phenyl-tolane isothiocyanate liquid crystal compounds. *Liq Cryst*. 2016;43:276–284.
- [12] Li JL, Li J, Hu MG, et al. The effect of locations of triple bond at terphenyl skeleton on the properties of isothiocyanate liquid crystals. *Liq Cryst*. 2017;44:1374–1383.
- [13] Jakub H, Jerzy D, Roman D, et al. Novel high birefringence isothiocyanates based on quaterphenyl and phenylethynyltolane molecular cores. *Liq Cryst*. 2013;40:1174–1182.
- [14] Dabrowski R, Dziaduszek J, Ziolk A, et al. Low viscosity, high birefringence liquid crystalline compounds and mixtures. *Opt-Electron Rev*. 2007;15:47–51.

- [15] Liao YM, Chen HL, Hsu CS, et al. Synthesis and mesomorphic properties of super high birefringence isothiocyanato bistolane liquid crystals. *Liq Cryst.* **2007**;34:507–517.
- [16] Arakawa Y, Kang SM, Tsuji H, et al. Development of novel bistolane-based liquid crystalline molecules with an alkylsulfanyl group for highly birefringent materials. *Rsc Adv.* **2016**;6:16568–16574.
- [17] Herman J, Kula P. Design of new super-high birefringent isothiocyanato bistolanes – synthesis and properties. *Liq Cryst.* **2017**;44:1462–1467.
- [18] Venkata Sai D, Sathyanarayana P, Sastry VSS, et al. Birefringence, permittivity, elasticity and rotational viscosity of ambient temperature, high birefringent nematic liquid crystal mixtures. *Liq Cryst.* **2014**;41:591–596.
- [19] Gauza S, Wen CH, Wu ST, et al. Super high birefringence isothiocyanato biphenyl-bistolane liquid crystals. *Jpn J Appl Phys.* **2004**;43:7634–7638.
- [20] Reuter M, Garbat K, Vieweg N, et al. Terahertz and optical properties of nematic mixtures composed of liquid crystal isothiocyanates, fluorides and cyanides. *J Mater Chem C.* **2013**;1:4457–4463.
- [21] Scherger B, Reuter M, Scheller M, et al. Discrete Terahertz beam steering with an electrically controlled liquid crystal device. *J Infrared Millim Terahertz Waves.* **2012**;33:1117–1122.
- [22] Spadlo A, Dabrowski R, Filipowicz M, et al. Synthesis, mesomorphic and optical properties of isothiocyanato-tolanes. *Liq Cryst.* **2003**;30:191–198.
- [23] Li JL, Li J, Hu MG, et al. New isothiocyanatotolane liquid crystals with terminal but-3-enyl substitute. *Liq Cryst.* **2017**;44:833–842.
- [24] Chen R, Weng Q, Wang L, et al. The effect of intermolecular actions on the nematic phase range of tolane-liquid crystals. *Liq Cryst.* **2017**. DOI:10.1080/02678292.2017.1402096.
- [25] Chen R, Zhao L, An ZW, et al. Synthesis and properties of allyloxy-based tolane liquid crystals with high negative dielectric anisotropy. *Liq Cryst.* **2017**;44:2184–2191.
- [26] Jiang Y, Lu LL, Chen P, et al. Synthesis and properties of allyloxy-based biphenyl liquid crystals with multiple lateral fluoro substituents. *Liq Cryst.* **2012**;39:957–963.
- [27] Catanesco CO, Chien LC. High birefringence nematic liquid crystals for display and telecom applications. *Mol Cryst Liq Cryst.* **2004**;411:93/[1135]–102/[1144].
- [28] Li J, Hu MG, Li JL, et al. Highly fluorinated liquid crystals with wide nematic phase interval and good solubility. *Liq Cryst.* **2014**;41:1783–1790.
- [29] Chen R, An ZW, Wang WL, et al. Lateral substituent effects on UV stability of high-birefringence liquid crystals with the diaryl-diacetylene core: DFT/TD-DFT study. *Liq Cryst.* **2017**;44:1515–1524.
- [30] Gauza S, Parish A, Wu ST, et al. Physical properties of laterally fluorinated isothiocyanato phenyl-tolane single liquid crystals components and mixtures. *Mol Cryst Liq Cryst.* **2008**;489:135–147.
- [31] Wang LY, Liao SS. *Liquid crystal chemistry*. Beijing: Science Press; **1988**. p. 65–73.
- [32] Chen R, Jiang Y, An ZW, et al. Dielectric and optical anisotropy enhanced by 1,3-dioxolane terminal substitution on tolane-liquid crystals. *J Mater Chem C.* **2015**;3:8706–8711.
- [33] Vuks MF. Determination of the optical anisotropy of molecules of aromatic compounds from the double refraction of crystals. *Opt Spectrosc.* **1966**;20:644–651.